The tip resistance in layered soils during static penetration

La résistance en pointe dans les sols stratifiés pendant une pénétration statique

Sturm H.
Norwegian Geotechnical Institute (NGI), Oslo, Norway

ABSTRACT: The maximum resistance during static penetration in layered soils is in general governed by the presence and properties of embedded granular layers; even so if these layers are thin compared to the dimensions of the penetrating object. In order to optimize the installation process as well as weight and geometry of the penetrating structure, it is important to assess reliably adequate strength parameters of these layers. By means of Finite Element calculations, normalized penetration resistance of a sand layer with varying properties embedded in soft clay have been determined. The results are presented in diagrams which can be used directly in a design.

RÉSUMÉ :La résistance des sols stratifiés pendant une pénétration statique dépend en général de la présence et des caractéristiques des couches granulaires, même si ces couches sont minces comparées aux dimensions de l'objet pénétrant. Afin d'optimaliser l'installation et le poids/géométrie d'une structure pénétrante, il est nécessaire d'établir de façon fiable les paramètres de résistance de chaque couche. La résistance à la pénétration normalisée pour une couche de sable entre deux couches d'argile molle a été établie par éléments finis. Les résultats sont présentés sous forme d'abaques qui peuvent être utilisées directement en dimensionnement.

KEYWORDS: Penetration resistance, thin sand layers, numerical simulations, hypoplasticity, parametric study.

1 INTRODUCTION AND MOTIVATION

The maximum resistance during static penetration in layered soils is in general governed by the presence and properties of embedded granular layers. The actual value of the resistance depends on the properties and state, i.e. density and stress, of the granular layers, as well as on the geometrical boundary condition, i.e. the relative thickness of the layers referred to the diameter of the penetrating object. Where relatively thin granular layers are present, the assessment of adequate strength parameters is a particular challenge, and there is always the danger of underestimating or overestimate the resistance, which can have significant impact on the design.

This paper presents a numerical parametric study where a thin sand layer embedded in soft clay has been analysed. Relative density and thickness of the sand, undrained shear strength of the surrounding clay and the vertical effective consolidation stress have been varied. The results are summarised in diagrams with normalised resistance factors. A simple procedure is proposed for superimposing the different influencing effects. This allows applying the results to a wide range of use cases; even to relatively thick sand layers where the state and properties may change with depth. Examples where the results of this study can be used are predicting the penetration resistance of prefabricated piles, bearing capacity of the tip of an installed pile and achievable penetration depth of dynamically installed torpedo piles (Sturm et al., 2011) to name but a few.

2 APPROACH AND ASSUMPTIONS

The relevance of size effects in the design are well known and were already studied previously by Vreugdenhil et al. (1994) using analytical methods, and Ahmadi and Robertson (2005) using numerical methods. Also in this study, a numerical approach has been adopted similar to the one proposed by Cudmani and Sturm (2006). With this model, they could predict qualitatively and quantitatively correct the mechanism and actual value of the tip resistance during static and dynamic penetration in both granular and soft soils.

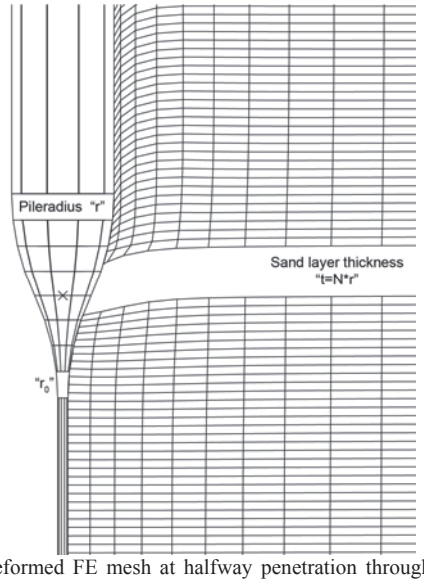

Figure 1 Deformed FE mesh at halfway penetration through the sand layer.

Figure 1 shows a detailed view of the tip of the axisymmetrical Finite Element (FE) mesh used in this study. The tip is somewhat rounded in order to improve the numerical stability of the contact formulation; the average opening angle, however, still corresponds to a CPT tip. To reduce excessive mesh distortion, a small initial opening gap under the tip of $r_0=r/10$ has been accounted for. Cudmani (2001) has shown that these modifications have only a small impact on the actual value

of the penetration resistance, but improve robustness and numerical stability, and allow large deformation FE simulations using implicit codes such Abaqus/Standard; which has been also used in the present study.

The width of the FE model amounts *100·r*, the height *(68+N)·r*, where *N* varies between *0.5* and *40* according to the considered thickness of the sand layer. Roller boundaries have been used at bottom and vertical outer boundary, while the free surface on top was charged with a constant surface load. The penetration calculation started with a tip "in-place" at *8·r* below the upper surface.

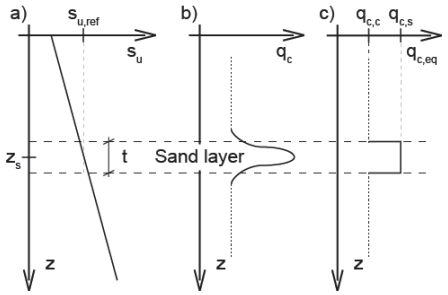

Figure 2 Linearization of soil properties and assessment of the equivalent tip resistance.

In order to make the results general applicable, a thin sand layer has been considered allowing linearising of state and soil properties as shown in Figure 2; meaning strength and stress have been assumed constant. To compare the different results of the parametric study, an equivalent tip resistance T^{eq}_{sand} of the sand layer has been determined by integrating the load-displacement curve and dividing it by the corresponding layer thickness; transition from b) to c) in Figure 2.

3 SIMULATIONS AND PARAMETRIC STUDY

The clay behaviour has been described with a linear elastic, perfectly plastic model using the Mohr-Coulomb failure criteria. For the sand, the hypoplastic model in the version proposed by von Wolffersdorff (1996) has been used, incorporating the intergranular strain extension proposed by Niemunis and Herle (1997). The parameters adopted are listed in Table 1.

Table 1 Hypoplastic and intergranular strain parameters of the sand layer.

φ_c	h_s	n	e_{d0}	e_{c0}	e_{i0}	α
32.8	625 [MPa]	0.33	0.67	1.05	1.21	0.18

β	m_2	m_5	R_{max}	β_χ	χ
1.12	2	2	0.001	0.1	1

The clay has been modelled undrained using a poison ratio of *0.495*. In the simulations where undrained conditions of the sand layers have been assumed, a bulk modulus of *2.2* GPa has been used for the pore water.

In order to prevent any affects of the vertical roller boundary on the penetration resistance due to the incompressibility of the clay, the FE model is divided vertically into two parts, where the outer part serves as a compensating layer. This layer has a poison ratio of *0.25*, or a bulk modulus of *0.0* GPa, respectively, and proportionally scaled properties with reduced stiffness. Sturm and Andresen (2010) have employed the same approach successfully for simulating the penetration and stress set-up of Torpedo Piles.

In the presented parametric study the following parameters have been varied (the values in brackets were adopted in the reference simulation used for the normalisation):

- Strength of the surrounding clay between *25* kPa and *250* kPa ($s_{u,ref}$=*50* kPa),
- Effective vertical consolidation stress between *50* kPa and *400* kPa (σ'_{ref}=*100* kPa) using k_0=*0.75*,
- Layer thickness between *0.5·r* and *40·r* (t_{ref}=*1·r*),
- And relative density between *25%* and *100%* ($D_{r,ref}$=*50%* which equates a void ratio of *e=0.86*).

4 RESULTS

Figure 3 shows the penetration resistance in a fully drained sand layer for constant stress, density and soil properties but different layer thicknesses. In addition the penetration resistance in sand or clay are plotted as upper and lower boundary, respectively.

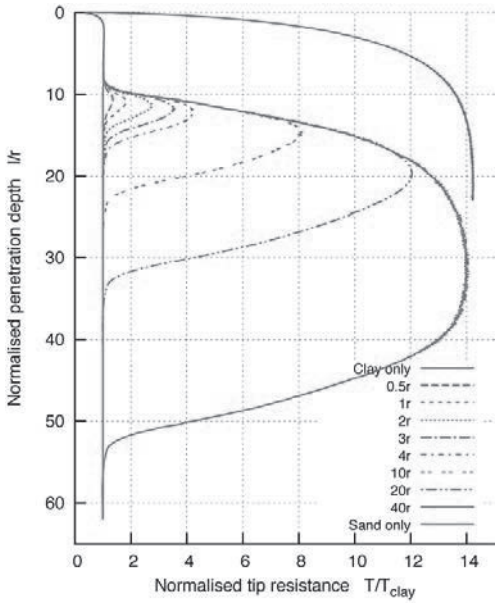

Figure 3 Tip resistance depending on the thickness of the drained sand layer. The results are normlised by the residual resistance in clay.

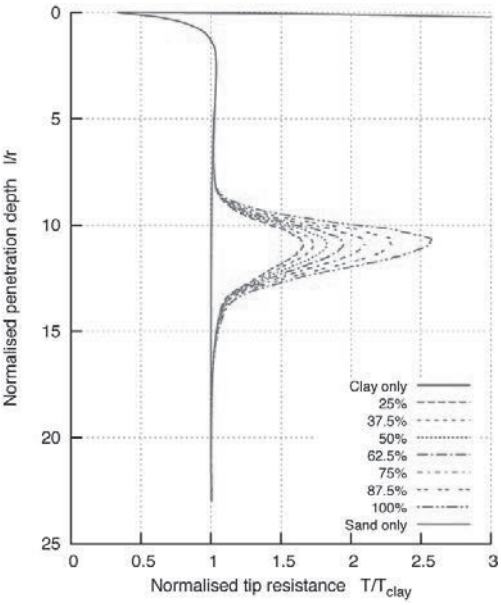

Figure 4 Tip resistance depending on the relative density of the drained sand layer. The results are normlised by the residual resistance in clay.

The shape of the curves are qualitatively similar to the analytical solutions proposed by Vreugdenhil et al. (1994) but are much smoother than the numerical simulations presented by Ahmadi and Robertsen (2005), which used an explicit FE code.

A layer thickness of more than *40·r* is required to reach the resistance of the sand layer. This agrees to the study from

Vreugdenhil at al. (1994), which indicated even a larger value of approximately $100 \cdot r$.

The stiffness of the sand layer is apparently independent of the layer thickness, which becomes evident from the congruent transition curves when approaching and penetrating the sand layer. An increase or decrease, respectively, of the stiffness can be seen, however, for varying relative densities as shown in Figure 4. A similar result is obtained when varying the clay strength and the vertical consolidation stress; not shown.

Figure 5 presents the equivalent tip resistance in drained sand normalised with the equivalent tip resistance of the reference simulation using the reference parameters listed in Section 3, viz.

$$\xi = \left(\frac{T^{eq}_{sand}}{T_{clay}}\right) / \left(\frac{T^{eq}_{sand}}{T_{clay}}\right)_{ref}$$

The equivalent strength of the drained sand layer in the reference model amounts $(T^{eq}_{sand}/T_{clay})_{ref}=3.44$.

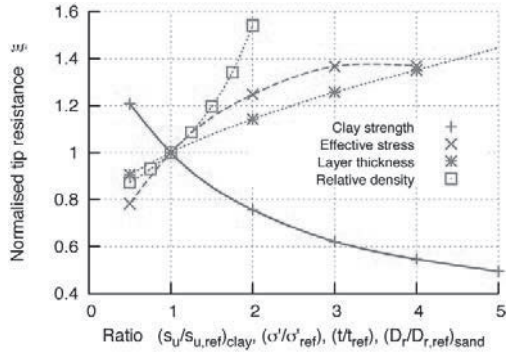

Figure 5 Normalised resistance of the drained sand layer depending on the shear strength of the clay, effective consolidation stress, thickness of the sand layer and relative density of the sand.

Figure 6 presents the normalised equivalent tip resistance in undrained sand normalized with the corresponding reference simulation using the same reference parameters.

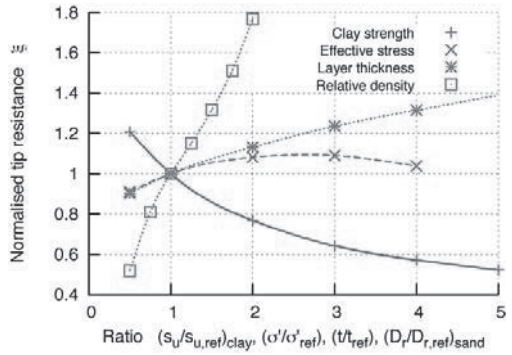

Figure 6 Normalised resistance of the undrained sand layer depending on the shear strength of the clay, effective consolidation stress, thickness of the sand layer and relative density of the sand.

The curves of the normalized resistances of both drained and undrained sand are very similar. Almost identical curves are obtained for varying shear strengths of the clay layer.

The effective consolidation stress has only a small influence on the resistance in undrained sand, which is plausible since the relative density governs the undrained strength of sand.

More pronounced is the effect of the relative density being larger under undrained conditions. The double-bended curve is somewhat unexpected. However, the resistances at low densities (*25%* and *37.5%*) are in practice less relevant. Noticeably, however, is, that the actual values are smaller than expected based on the diagrams proposed Baldi et al. (1986). But since the tip resistance in pure sand as measured by Baldi et al. (1986) can be well reproduced by the FE model using the hypoplastic formulation (Cudamni and Sturm, 2006), it is believed that the lower normalised relative resistances at high relative densities are affected by the layer thickness. The sand is squeezed horizontally but also vertically into the softer clay which results in a lower resistance. The squeezing can be well seen in the deformed mesh when high densities and low undrained shear strengths for the clay are used. In some cases it lead to distorted elements introducing numerical difficulties. These simulations have not been included in the presented diagrams. The vertical squeezing explains also the higher resistances under undrained conditions compared to drained conditions. The excess pore pressure is less than during penetration in pure undrained sand with similar properties, resulting in higher effective stresses under the tip and hence higher penetration resistance.

In case of very thin to thin layers, the effect of the thickness on the penetration resistance is almost independent of the drainage conditions of the sand. However, when plotting these curves over a larger range, as shown in Figure 7, it becomes apparent that the effect is larger under drained conditions. In addition the theoretical residual maximum normalised resistance for drained and undrained conditions are plotted in Figure 7. The curves approaching the theoretical values only asymptotically, but it is reasonable to assume a value of approximately $80 \cdot r$ to $100 \cdot r$ as an upper limit at which a further increase of the thickness has a negligible effect on the equivalent resistance.

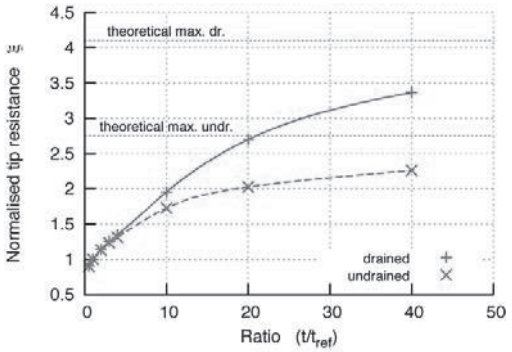

Figure 7 Normalised resistance of the drained and undrained sand layer depending in the layer thickness.

5 APPLICATION RANGE AND LIMITATIONS

5.1 *Application*

In order to use the results shown in Figure 5 to Figure 7 for other design cases than the ones simulated, the different normalised resistance factors just need to be multiplied. For example, the normalised resistance of a drained sand layer with $s_{u,clay}=12.5$ kPa, $\sigma'_v=200$ kPa, $t=2 \cdot r$ and $Dr=100\%$ is $\xi=1.21 \cdot 1.25 \cdot 1.14 \cdot 1.54=2.66$ or $T^{eq}_{sand}=3.44 \cdot 2.66=9.15 \cdot T_{clay}$, respectively, where $T_{clay}=N_c \cdot \pi r^2 \cdot s_{u,clay}$ with $s_{u,clay}=12.5$ kPa. This value agrees well with the result of a corresponding FE calculation.

The plausibility of this approach becomes apparent from the following simple example: considering two drained sand layers with equal density and thickness embedded in normal consolidated clay but at different depths. The vertical effective stress and the strength of the normal consolidated clay increase linearly with depth. The equivalent tip resistance should be then almost equal in both sand layers, meaning that both effects should cancel out, given that the sand resistance is stress independent. This, however, is not the case in the hypoplastic formulations. Thus, the resistances are only approximately similar within a range of $\pm 50\%$.

In practice, the diagrams are used to estimate the scaling effects and to provide input for sensitivity studies. Starting point in most cases will be a CPT profile indicating the presence of a

sand layer, for which an appropriate equivalent resistance needs to be assessed for the considered design case of the structure.

Where soil and state properties cannot be linearised, an upper and lower equivalent resistance can be assessed using the diagrams. The resistance can be then interpolated linearly between both values. Due to the squeezing effect,, the scaling factors accounting for changes in relative density, shown in Figure 5 and Figure 6, may underestimate the actual resistance of relatively thick layers. Thus, the diagrams proposed by Baldi et al. (1986) might be used instead.

In order to consider different penetration rates, meaning partially drained conditions of the sand layer, a fully drained and a fully undrained equivalent resistance need to be determined. Given that the drainage and hydraulic boundary conditions are comparable between the reference test, e.g. a CPT measurement, and the structure to be designed, one can interpolate between the two values using one of the approaches discussed by Danziger and Lunne (2012).

The diagrams can be also used where viscous-type rate effect matters. In this case the penetration rate used in the soil investigation should corresponds to the penetration rate of the structure to be designed.

5.2 *Limitations*

The diagrams cannot be directly used for multi-layered soils where sand layers interfere with each other, meaning that the resistance in the clay is affected by both an upper and a lower granular layer.

In this study, a stress ratio of $k_0=0.75$ has been used. The diagrams can be employed to other stress case only, when the stress state is corrected for the effective mean stress, which governs the response of the sand layer in the hypoplastic formulation. Preliminary FE calculations indicate that the curves are very similar to ones presented in Figure 5 to Figure 7. However, further calculations needs to be performed to confirm that.

Only one sand type has been considered in the presented parametric study. Due to the normalisation, the diagrams should be applicable to other sands as well. FE simulations, in which other soil properties for the sand have been used, showed quantitatively similar curves. However, additional simulations should be performed to confirm the normalisation and the general applicability of the diagrams to other materials.

Not considered by the hypoplastic model is grain crushing. At high penetration pressures, grains may crush, which is accompanied by a change of the soil properties. Although FE calculations indicate that the diagrams are applicable to other sands with different properties than the one analysed, the properties should not change during penetration. Grain crushing affects the grain size distribution and the limiting void ratios, meaning that for example also the relative density changes. Thus, the diagrams cannot be applied when grain crushing is expected.

6 SUMMARY AND OUTLOOK

In this contribution, the effect of thin sand layers on the penetration resistance is discussed. By means of FE simulations, a comprehensive parametric study has been performed varying thickness and relative density of a sand layer embedded in soft clay. In addition, the strength of the clay and the vertical consolidation stress has been systematically varied. The results are presented in normalised diagrams of which the influencing factors can be read out. To superimpose different effects, the corresponding factors need to be simply multiplied. The plausibility of this approach has been shown and possible application cases have been discussed.

To overcome some of the limitations and existing uncertainties, further FE simulations are planned to perform, in which in particular the stress ratio k_0 and the soil properties are varied systematically. It is believed that different soil properties do not affect the presented diagrams and the effect of the stress ratio can be represented by an additional normalised curve.

In addition to numerical studies, model and field tests should be performed to reinforce the approach proposed.

7 REFERENCES

Ahmadi M.M. and Robertson P.K. 2005. *Thin-layer effects on the CPT q_c measurement*. Can. Geotech. J. 42: 1302-1317.

Baldi G., Belotti R., Ghionna N., Jamiolkowski M. and Pasqualini E. (1986), *Interpretation of CPT's and CPTU's. 2nd Part: Drained penetration resistance*. 4th International Geotechnical Seminar, Field Instrumentation and In-Situ Measurements, Singapore, 143-153

Cudmani R. 2001. *Statische, alternierende und dynamische Penetration nichtbindiger Böden*. Ph.D thesis, Karlsruhe, Germany.

Cudmani R. and Sturm H. 2006. *An investigation of the tip resistance in granular and soft soils during static, alternating and dynamic penetration*. Int. Sym. on vibratory pile driving and deep soil compaction TRANSVIB 2006, Paris, France.

Danziger F. and Lunne T. (2012), *Rate effect on cone penetration test in sand*, Geotechnical Engineering Journal of the SEAGS & AGSSEA Vol. 43 No. 4, 72-81

Niemunis A. and Herle I. (1997), *Hypoplastic model for cohesionless soils with elastic strain range*, Mechanics of Cohesive-Frictional Materials, Vol. 2, 279-299

Sturm H. and Andresen L. 2010. *Large deformation analysis of the installation of dynamic anchors*. NUMGE 2010, Trondheim, Norway.

Sturm H., Lieng J.T. and Saygili G. 2011. *Effect of soil variability on the penetration depth of dynamically installed drop anchors*. OTC Brasil 2011, Rio de Janeiro, *OTC 22396*.

Vreugdenhil R. Davis B. and Berrill J. 1994. *Interpretation of cone penetration results in multilayered soils*. Int. J. Num. Ana. Methods, Vol. 18: 585-599.

Wolffersdorff P.-A. v. (1996), *A hypoplastic relation for granular material with predefined limit state surface*, Mechanics of Cohesive-Frictional Materials, Vol. 1, No. 3, 251-275